

QUANTUM MONTE CARLO METHODS FOR NUCLEI

BY ROBERT B. WIRINGA

A major goal in nuclear physics is to understand how nuclear binding, structure, and reactions can be described from the underlying interactions between individual nucleons^[1,2]. We want to compute the properties of an A -nucleon system as an A -body problem with free-space nuclear interactions that describe nucleon-nucleon (NN) scattering and the two-nucleon bound-state. Properties of interest for a given nucleus include the ground-state binding energy, excitation spectrum, one- and two-nucleon density and momentum distributions, electromagnetic moments and transitions. We also wish to describe the interactions of nuclei with electrons, neutrinos, pions, nucleons, and other nuclei. Such calculations can provide a standard of comparison to test whether sub-nucleonic effects, such as explicit quark degrees of freedom, must be invoked to explain an observed phenomenon. They can also be used to evaluate nuclear matrix elements needed for some tests of the standard model, and to predict reaction rates that are difficult or impossible to measure in the laboratory. For example, all the astrophysical reactions that contribute to the Big Bang or to solar energy production should be amenable to such *ab initio* calculations.

To achieve this goal, we must both determine reasonable Hamiltonians to be used and devise reliable many-body methods to evaluate them. Significant progress has been made in the past decade on both fronts, with the development of a number of potential models that accurately reproduce NN elastic scattering data, and a variety of advanced many-body methods. In practice, to reproduce experimental energies and transitions, it appears necessary to add many-nucleon forces to the Hamiltonian and electroweak charge and current operators beyond the basic single-nucleon terms. While testing our interactions and currents against experiment, it is also important to test the many-body methods against each other to ensure that any approximations made are not biasing the results.

For s -shell (3- and 4-body) nuclei, a number of accurate many-body methods have been developed; a benchmark test in 2001 compared seven different calculations of the

binding energy of the ${}^4\text{He}$ nucleus using a semi-realistic test Hamiltonian and obtained agreement at $\approx 0.1\%$ ^[3]. Multiple few-body methods also agree quite well on low-energy three-nucleon ($3N$) scattering and progress is being made on larger scattering problems^[4,5]. For p -shell ($5 \leq A \leq 16$) and larger nuclei, three methods that are being developed and checked against each other are the no-core shell model (NCSM)^[6], coupled-cluster expansion (CCE)^[7], and quantum Monte Carlo (QMC)^[2]. This article will focus on the quantum Monte Carlo method as an example of modern *ab initio* nuclear theory. We will describe the nature of the problem, a method of solution, and present some of the successes that have been achieved as well as future challenges that must be faced.

NUCLEAR HAMILTONIAN

At present we have to rely on phenomenological models for the nuclear interaction; a quantitative understanding of the nuclear force based on non-perturbative quantum chromodynamics (QCD) is still some distance in the future. We consider nuclear Hamiltonians of the form:

$$H = \sum_i K_i + \sum_{i<j} v_{ij} + \sum_{i<j<k} V_{ijk}.$$

Here K_i is the kinetic energy, v_{ij} is an NN potential, and V_{ijk} is a $3N$ potential. Realistic NN potentials fit a large scattering database; models such as the Nijm I, Nijm II, and Reid93 potentials of the Nijmegen group^[8], Argonne v_{18} (AV18)^[9], and CD Bonn^[10], fit more than 4,000 elastic data at laboratory energies ≤ 350 MeV with a $\chi^2/\text{datum} \sim 1$. These potentials are all based on pion exchange at long range, but inevitably are more phenomenological at shorter distances. Their structure is complicated, including spin, isospin, tensor, spin-orbit, quadratic momentum-dependent, and charge-independence-breaking terms, with ~ 40 fitted parameters. However, these sophisticated NN models are generally unable to reproduce the binding energy of few-body nuclei such as ${}^3\text{H}$ and ${}^4\text{He}$ without the assistance of a $3N$ potential^[11].

Multi-nucleon interactions can arise because of the composite nature of the nucleon and its corresponding excitation spectrum, particularly the strong $\Delta(1232)$ resonance seen in πN scattering. The expectation value of $3N$ potentials is much smaller than that for NN forces, but due to the large cancellation between one-body kinetic and two-body potential energies, they can provide significant corrections to nuclear binding. Fortunately, four-nucleon potentials



R.B. Wiringa
<wiringa@anl.gov>, Physics Division, Argonne National Laboratory, Argonne, Illinois 60439

SUMMARY

Quantum Monte Carlo methods are applied to the *ab initio* calculation of the structure and reactions of light nuclei.



appear small enough to ignore at present. Models for the basic two-pion-exchange $3N$ potential date from the 1950s [11]; more sophisticated models have followed, including the Tucson-Melbourne [12], Urbana [13], and Illinois [14] models. In principle, the $3N$ potential could have a far more complicated dependence on the spins, isospins, and momenta of the nucleons than has been studied to date, but there is limited information by which to constrain the models. Three-nucleon scattering data provides some information, but very little partial-wave analysis has been done which would help unravel the structure. Energies and excitation spectra of light nuclei provide the best current constraints for $3N$ potentials, especially isospin $T = \frac{1}{2}$ interactions, which are particularly important for neutron stars. Hamiltonians based on chiral effective theories are under development that should provide a more consistent picture of both NN and many-nucleon forces, while also making closer connections to the underlying symmetries of QCD [15].

An important additional ingredient for the evaluation of electroweak interactions of nuclei is a consistent set of charge and current operators. The standard impulse approximation (IA) single-nucleon contributions need to be supplemented by many-nucleon terms that again can be understood as arising from the composite nature of the nucleons and the meson exchanges that mediate the interactions between them. It is important to use currents that satisfy the continuity equation with the Hamiltonian. In practice, two-nucleon operators give the bulk of the correction to the IA terms; they can be 20% corrections for magnetic moments and transitions, although generally much less for electric transitions and weak decays [1].

For the present article, we consider a Hamiltonian containing the AV18 NN potential and Illinois-2 (IL2) $3N$ potential. The AV18 model can be written in an operator format as:

$$v_{ij} = \sum_{p=1,22} v_p(r_{ij}) O_{ij}^p,$$

$$O_{ij}^{p=1,14} = [1, \sigma_i \cdot \sigma_j, S_{ij}, \mathbf{L} \cdot \mathbf{S}, \mathbf{L}^2, \mathbf{L}^2 \sigma_i \cdot \sigma_j, (\mathbf{L} \cdot \mathbf{S})^2] \otimes [1, \tau_i \cdot \tau_j],$$

$$O_{ij}^{p=15,22} = [1, \sigma_i \cdot \sigma_j, S_{ij}, \mathbf{L} \cdot \mathbf{S}] \otimes [T_{ij}, (\tau_{zi} + \tau_{zj})].$$

Here σ (τ) is the Pauli spin (isospin) operator, \mathbf{L} (\mathbf{S}) is the pair orbital (spin) angular momentum operator, and $S_{ij} = 3\sigma_i \cdot \hat{\mathbf{r}}_{ij} \sigma_j \cdot \hat{\mathbf{r}}_{ij} - \sigma_i \cdot \sigma_j$ is the tensor operator, which can exchange spin and orbital angular momenta. The first fourteen terms are isoscalar, or charge-independent, i.e., they do not mix isospin states. The first eight of these terms, up through spin-orbit, are the most important. A good semi-realistic model designated AV8' has been constructed (and used in the ${}^4\text{He}$ benchmark paper mentioned above) using just these operators; it reproduces S - and P -wave NN scattering phase shifts and the two-nucleon bound state (deuteron) very well. The central, spin-isospin, and tensor-isospin components are shown in Fig. 1 by solid lines with the left-hand scale; the central potential has its maximum of ≈ 2000 MeV at $r = 0$.

The six terms quadratic in \mathbf{L} are smaller, but are needed to fit higher partial waves in NN scattering. The last eight terms

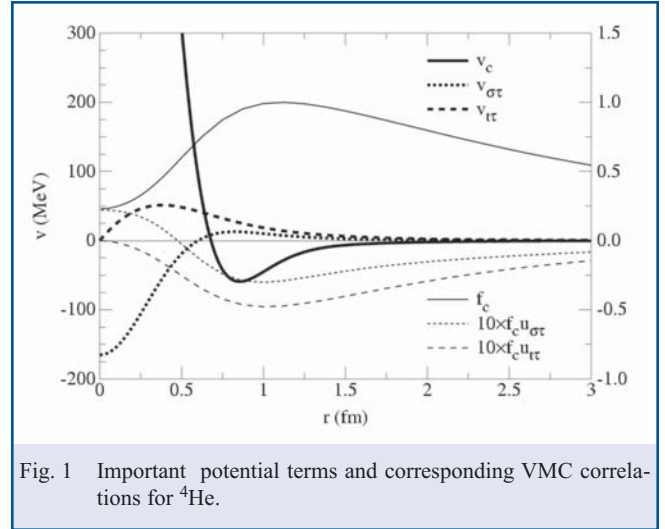


Fig. 1 Important potential terms and corresponding VMC correlations for ${}^4\text{He}$.

break charge-independence, being either isovector ($\tau_{zi} + \tau_{zj}$), or isotensor ($T_{ij} = 3\tau_{zi}\tau_{zj} - \tau_i \cdot \tau_j$), in character; they are generally small, and differentiate between pp , np and nm forces. Their origin is in the electromagnetic (Coulomb, magnetic moment, etc.) interaction, and the strong interaction ($m_{\pi^0} - m_{\pi^\pm}$ effects, ρ - ω meson mixing, etc.).

The IL2 $3N$ potential includes a long-range two-pion-exchange piece, three-pion-exchange ring terms, and a phenomenological short-range repulsion. The spin- and isospin-dependence is fixed by the rules of πN interactions, while the overall strength is characterized by four parameters determined by a fit to ~ 20 nuclear energy levels when used with AV18 in the calculations described below.

QUANTUM MONTE CARLO METHODS

The many-body problem with the full Hamiltonian described above is uniquely challenging. We want to solve the many-body Schrödinger equation

$$H \Psi(\mathbf{r}_1, \mathbf{r}_2, \dots, \mathbf{r}_A; s_1, s_2, \dots, s_A; t_1, t_2, \dots, t_A) = E \Psi(\mathbf{r}_1, \mathbf{r}_2, \dots, \mathbf{r}_A; s_1, s_2, \dots, s_A; t_1, t_2, \dots, t_A)$$

where $s_i = \pm \frac{1}{2}$ are nucleon spins, and $t_i = \pm \frac{1}{2}$ are nucleon isospins (proton or neutron). This is equivalent to solving, for an A -body nucleus with Z protons, $2^A \times \binom{A}{Z}$ complex coupled second-order differential equations in $3A$ -dimensions. For ${}^{12}\text{C}$, this number is 3,784,704 coupled equations in 36 variables! (In practice, for many nuclei, symmetry considerations can reduce the number by an order of magnitude.) The coupling is quite strong; the expectation value $\langle v_{\tau\tau} \rangle$ corresponding to the tensor-isospin operator $S_{ij}\tau_i \cdot \tau_j$ is $\approx 60\%$ of $\langle v_{ij} \rangle$. This is a direct consequence of the pion-exchange nature of nuclear forces (and indirectly, the approximate chiral symmetry of QCD). Furthermore, $\langle v_{\tau\tau} \rangle = 0$ if there are no tensor correlations in the wave function, so we cannot perturbatively introduce these couplings.

The first application of Monte Carlo methods to nuclei interacting with realistic potentials was a variational (VMC) calculation by Pandharipande and collaborators [16], who computed upper bounds to the binding energies of ^3H and ^4He in 1981. Six years later, Carlson [17] improved on the VMC results by using the Green's function Monte Carlo (GFMC) algorithm, obtaining essentially exact results (within Monte Carlo statistical errors of 1%). Reliable calculations of light p -shell nuclei started to become available in the mid 1990s and are reviewed in [2]; the most recent results for $A = 9, 10$ nuclei and ^{12}C can be found in [18, 19].

A VMC calculation finds an upper bound E_V to an eigenenergy E_0 of the Hamiltonian by evaluating the expectation value of H in a trial wave function, Ψ_T :

$$E_V = \frac{\langle \Psi_T | H | \Psi_T \rangle}{\langle \Psi_T | \Psi_T \rangle} \geq E_0.$$

Parameters in Ψ_T are varied to minimize E_V , and the lowest value is taken as the approximate energy. A good trial function is [2]

$$|\Psi_T\rangle = \left[1 + \sum_{i < j < k} U_{ijk} \right] \left[S \prod_{i < j} (1 + U_{ij}) \right] |\Psi_J\rangle,$$

where U_{ij} and U_{ijk} are non-commuting two- and three-body correlation operators induced by v_{ij} and V_{ijk} , respectively, S is a symmetrizer, and the Jastrow wave function Ψ_J is

$$|\Psi_J\rangle = \prod_{i < j} f_c(r_{ij}) |\Phi_A(J^\pi; T)\rangle.$$

Here the single-particle A -body wave function $\Phi_A(J^\pi; T)$ is fully antisymmetric and has the total spin, parity, and isospin quantum numbers of the state of interest, while the product over all pairs of the central two-body correlation $f_c(r_{ij})$ keeps nucleons apart to avoid the strong short-range repulsion of the interaction. The long-range behavior of f_c and any single-particle radial dependence in Φ_A (which is written using coordinates relative to the center of mass or to a sub-cluster CM to ensure translational invariance) control the finite extent of the nucleus.

The two-body correlation operator has the structure

$$U_{ij} = \sum_{p=2,6} u_p(r_{ij}) O_{ij}^p,$$

where the O_{ij}^p are the leading spin, isospin, and tensor operators in v_{ij} . The $f_c(r)$ and $u_p(r)$ are obtained by numerically solving a set of six Schrödinger-like equations: two single-channel for $S=0$, $T=0$ or 1, and two coupled-channel for $S=1$, $T=0$ or 1, with the latter producing the important tensor correlations [20]. These equations contain the bare v_{ij} and parametrized Lagrange multipliers to impose long-range boundary conditions of exponential decay and tensor/central ratios.

The central, spin-isospin, and tensor-isospin correlations obtained for ^4He are shown in Fig. 1 as dashed lines measured by the right-hand scale. The f_c is small at short distances, to reduce contributions from the repulsive core of v_c , and a maximum near where v_c is most attractive, while the long-range decrease keeps the nucleus confined. The $u_{\sigma\tau}$ and u_{τ} are small and have signs opposite to $v_{\sigma\tau}$ and v_{τ} as expected from perturbation theory.

Perturbation theory is also used to motivate the three-body correlation $U_{ijk} = -\varepsilon V_{ijk}(\tilde{r}_{ij}, \tilde{r}_{jk}, \tilde{r}_{ki})$ where $\tilde{r} = yr$, y a scaling parameter, and ε a (small negative) strength parameter. Consequently, U_{ijk} has the same spin, isospin, and tensor dependence that V_{ijk} contains.

The Ψ_T is a vector in the spin-isospin space of the A nucleons, each component of which is a complex-valued function of the positions of all A nucleons. The tensor correlations mix spin and spatial angular momenta, so that all 2^A spin combinations appear. Because the nuclear force is mostly isoscalar, the conservation of isospin results in fewer isospin possibilities, somewhat less than $\binom{A}{2}$. For $M_J = 0$ states there is an additional factor of 2 reduction. The total numbers of components in the vectors for ^4He , ^6Li , ^8Be , ^{10}B , and ^{12}C are 16, 160, 1792, 21504, and 270336, respectively.

Constructing the trial function with the pair spin and isospin operators in U_{ij} requires $P = A(A-1)/2$ sparse-matrix operations on this vector (more if U_{ijk} triples are used). Acting on the trial function with v_{ij} then requires a sum of P additional operations for each spin or isospin term in the potential. Kinetic energy contributions are evaluated by finite differences, i.e., by reconstructing Ψ_T at $6A$ slightly shifted positions and taking appropriate differences. Quadratic momentum-dependent \mathbf{L}^2 and $(\mathbf{L}\cdot\mathbf{S})^2$ terms in v_{ij} require additional derivatives, but various tricks can be used to reduce the number of operations, including rotation to a frame where fewer differences are needed, and Monte Carlo sampling these relatively short-ranged terms when the two nucleons are far apart. Evaluating V_{ijk} requires additional operations, but these terms can also be sampled when the nucleons are far apart. The $3A$ -dimensional spatial integration is carried out by a standard Metropolis Monte Carlo algorithm [21] with sampling controlled by a weight function $W(\mathbf{R}) \approx |\Psi_T|^2$, where $\mathbf{R} = \mathbf{r}_1, \mathbf{r}_2, \dots, \mathbf{r}_A$ specifies the spatial configuration. Thus more (less) time is spent evaluating the integral where the trial function is large (small).

VMC calculations produce upper bounds to binding energies that are $\approx 2\%$ above exact results for $A = 3, 4$ nuclei. However, as A increases, our present trial functions get progressively worse and are unstable against breakup into sub-clusters. For example, our ^7Li trial function is more bound than ^6Li , but less bound than ^4He plus ^3H . Because any wave function can be expanded in the complete set of exact eigenfunctions, the inadequacy of the trial function can be attributed to contamination by excited state components in Ψ_T .

The Green's function Monte Carlo method provides a way of systematically improving on the VMC trial state by removing such contamination and approaching the true lowest-lying eigenstate of given $(J^\pi; T)$ quantum numbers [2]. GFMC projects out the lowest-energy eigenstate from Ψ_T by a propagation in imaginary time:

$$\begin{aligned} \Psi(\tau) &= \exp[-(H - \tilde{E}_0)\tau]\Psi_T, \\ &= e^{-(E_0 - \tilde{E}_0)\tau} \times [\Psi_0 + \sum \alpha_i e^{-(E_i - E_0)\tau} \Psi_i], \\ \lim_{\tau \rightarrow \infty} \Psi(\tau) &\propto \Psi_0, \end{aligned}$$

where \tilde{E}_0 is a guess for the exact E_0 . If sufficiently large τ is reached, the eigenvalue E_0 is calculated exactly while other expectation values are generally calculated neglecting terms of order $|\Psi_0 - \Psi_T|^2$ and higher. In contrast, the error in the variational energy, E_V , is of order $|\Psi_0 - \Psi_T|^2$, and other expectation values calculated with Ψ_T have errors of order $|\Psi_0 - \Psi_T|$.

The evaluation of $e^{-(H - \tilde{E}_0)\tau}$ is made by introducing a small time step, $\Delta\tau = \tau/n$ (typically $\Delta\tau = 0.0005 \text{ MeV}^{-1}$),

$$\Psi(\tau) = \left[e^{-(H - \tilde{E}_0)\Delta\tau} \right]^n \Psi_T = G^n \Psi_T.$$

where G is the short-time Green's function. Again, $\Psi(\tau)$ is a vector function of \mathbf{R} , and the Green's function $G_{\alpha\beta}(\mathbf{R}', \mathbf{R})$ is a matrix function of \mathbf{R} and \mathbf{R}' in spin-isospin space:

$$G_{\alpha\beta}(\mathbf{R}', \mathbf{R}) = \left\langle \mathbf{R}', \alpha \left| e^{-(H - \tilde{E}_0)\Delta\tau} \right| \mathbf{R}, \beta \right\rangle$$

where α, β denote the spin-isospin components. The repeated operation of $G_{\alpha\beta}(\mathbf{R}', \mathbf{R})$ in coordinate space results in a multi-dimensional integral over $3An$ (typically more than 10,000) dimensions. This integral is also done by a Metropolis Monte Carlo algorithm.

The short-time propagator is approximated as a symmetrized product of exact two-body propagators and includes the $3N$ potential to first-order. The $G_{\alpha\beta}(\mathbf{R}', \mathbf{R})$ can be evaluated with leading errors of order $(\Delta\tau)^3$, which can be made arbitrarily small by reducing $\Delta\tau$ (and increasing n correspondingly). In the benchmark calculation [3] of ${}^4\text{He}$, the GFMC energy had a statistical error of only 20 keV and agreed with the other best results to this accuracy ($< 0.1\%$). Various tests indicate that the GFMC calculations of p -shell binding energies have errors of 1–2%.

For more than four nucleons, GFMC calculations suffer significantly from the well-known fermion sign problem; the $G_{\alpha\beta}(\mathbf{R}', \mathbf{R})$ is a local operator that does not know about global antisymmetry. Consequently it can mix in boson solutions that are generally (much) lower in energy. This results in exponential growth of the statistical errors as one propagates to larger τ , or as A is increased. For $A \geq 8$ the resulting limit on τ is too small to allow convergence of the energy. This problem is solved by using a constrained-path algorithm [22], in which configurations with small or negative $\Psi(\tau)^\dagger \cdot \Psi_T$ are discarded

such that the average over all discarded configurations of $\Psi(\tau)^\dagger \cdot \Psi_T$ is 0. Thus, if Ψ_T were the true eigenstate, the discarded configurations would contribute nothing but noise to $\langle H \rangle$. In practice, a final few (10–20) unconstrained steps are made, before evaluating the energy, to eliminate any bias from the constraint.

Expectation values with GFMC wave functions are evaluated as “mixed” estimates

$$\langle O(\tau) \rangle_{\text{Mixed}} = \frac{\langle \Psi(\tau) | O | \Psi_T \rangle}{\langle \Psi(\tau) | \Psi_T \rangle}.$$

The desired expectation values would have $\Psi(\tau)$ on both sides, but if the starting trial wave function is reasonably good, we can write $\Psi(\tau) = \Psi_T + \delta\Psi(\tau)$, and neglecting terms of order $[\delta\Psi(\tau)]^2$, we obtain the approximate expression

$$\langle O(\tau) \rangle = \frac{\langle \Psi(\tau) | O | \Psi(\tau) \rangle}{\langle \Psi(\tau) | \Psi(\tau) \rangle} \approx \langle O(\tau) \rangle_{\text{Mixed}} + [\langle O(\tau) \rangle_{\text{Mixed}} - \langle O \rangle_V],$$

where $\langle O \rangle_V$ is the variational expectation value. More accurate evaluations of $\langle O(\tau) \rangle$ are possible, essentially by measuring the observable at the mid-point of the path. However, such estimates require a propagation twice as long as the mixed estimate and require separate propagations for every $\langle O \rangle$ to be evaluated.

In practice, the operator in the mixed estimate acts on the explicitly antisymmetric Ψ_T , which helps project out boson contamination in $\Psi(\tau)$ and is particularly convenient for evaluating operators with derivatives. The expectation value of the Hamiltonian is a special case, because half of the propagator can be commuted to the other side of the mixed expectation value, giving $\Psi(\tau/2)$ on either side; consequently the energy has a variational upper bound property and converges to the eigenenergy from above.

As described above, the number of spin-isospin components in Ψ_T grows rapidly with the number of nucleons. Thus, a calculation of a state in ${}^8\text{Be}$ involves about 30 times more floating-point operations than one for ${}^6\text{Li}$, and ${}^{10}\text{B}$ requires 25 times more than ${}^8\text{Be}$. Calculations of the sort being described are currently feasible for $A \leq 10$. A few runs for the ground state of ${}^{12}\text{C}$ have been made; these require $\sim 100,000$ processor hours on modern massively parallel computers or $\sim 10^{17}$ floating point operations for a single state.

RESULTS

The imaginary-time evolution of GFMC calculations for the first three $(J^\pi; T=0)$ states in ${}^6\text{Li}$ is shown in Fig. 2. The energy is evaluated after every $40\Delta\tau$ propagation steps and is shown by the solid symbols with error bars for the Monte Carlo statistical errors. The $E_V = E(\tau = 0)$ for the 1^+ ground state is at -28 MeV , above the threshold for breakup into separated $\alpha({}^4\text{He})$ and deuteron (${}^2\text{H}$) clusters. However, the energy drops quite rapidly and is already stable against breakup after only a few

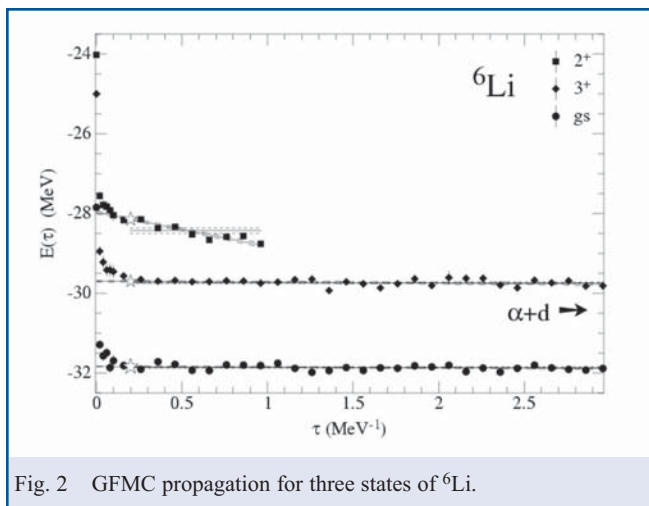


Fig. 2 GPMC propagation for three states of ${}^6\text{Li}$.

propagation steps. The final energy and statistical error is obtained by averaging over $E(\tau)$ once the energy is stable. The rapid drop in $E(\tau)$ for small τ indicates that the Ψ_T has a small contamination of very high (>100 MeV) excitation; GPMC is particularly efficient at filtering out such errors.

The 3^+ excited state is actually unstable against cluster breakup, but is physically narrow (decay width $\Gamma=0.024$ MeV) and the GPMC energy is stable. However, the 2^+ excited state is physically wide ($\Gamma=1.3$ MeV) and after an initial rapid drop from the -24 MeV starting energy, it continues to drift lower, so a straight average is not reasonable. In principle, if the calculation is carried to large enough τ , the energy should converge to the sum of α and deuteron energies. In this case we extrapolate linearly back to the end of the initial drop as marked by the open star in Fig. 2 to estimate the energy of the state.

Figure 3 compares GPMC calculations of energy levels of selected nuclei with the experimental values (right bars). The calculations use just the AV18 NN potential alone (left bars) or with the IL2 $3N$ potential (middle bars). The figure shows that calculations with just a NN potential underbind the $A \geq 3$ nuclei, with the underbinding getting worse as A increases. In addition many spin-orbit splittings, such as that of the $\frac{5}{2}^- - \frac{7}{2}^-$ levels in ${}^7\text{Li}$, are too small. The addition of IL2 corrects these errors and results in good agreement with the data; for 53 levels in $3 \leq A \leq 10$ nuclei the rms deviation from experiment is only 740 keV. The case of ${}^{10}\text{B}$ is particularly interesting, as the calculation with just AV18 incorrectly produces a 1^+ ground state instead of the correct 3^+ . As the figure shows, including IL2 reverses the order of the two levels and produces the correct ground state. This result has been confirmed by NCSM calculations using different realistic NN and $3N$ potentials [23].

Many of the states shown in Fig. 3 are strong stable, i.e., they can decay only by electromagnetic or weak transitions, if at all. Others are actually resonant states that decay by nucleon or α emission. As discussed above, good energies can still be

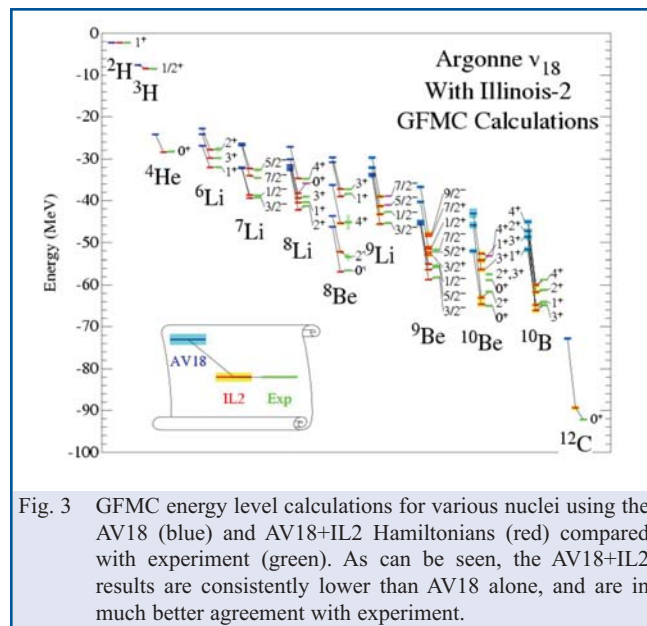


Fig. 3 GPMC energy level calculations for various nuclei using the AV18 (blue) and AV18+IL2 Hamiltonians (red) compared with experiment (green). As can be seen, the AV18+IL2 results are consistently lower than AV18 alone, and are in much better agreement with experiment.

obtained for resonant states that are physically narrow by the techniques discussed above, but for wide states with decay widths $\Gamma > 0.2$ MeV, a true scattering calculation is more appropriate.

A nuclear GPMC calculation was recently completed for the case of $n+\alpha$ scattering [24]. The basic technique is to confine the nucleons in a box, with a radius large enough so that a nucleon at the edge is far enough away from the others (inside the α) that it is in the asymptotic scattering regime. A logarithmic boundary condition is imposed on the trial function, and a GPMC propagation is made that preserves the boundary condition while finding the energy of the system. The combination of energy and logarithmic derivative at the boundary radius gives a phase shift $\delta(E)$. A number of calculations are made for different boundary conditions to map out $\delta(E)$, from which partial-wave cross sections can be calculated and resonance poles and widths extracted. This is illustrated in Fig. 4, where $n+\alpha$ scattering in the $\frac{1}{2}^+$, $\frac{1}{2}^-$, and $\frac{3}{2}^-$ channels, calculated with AV18+IL2, is plotted (solid symbols) and compared to an R -matrix analysis of experimental data (solid lines). The agreement is quite encouraging, but this is by far the simplest of many scattering cases we would like to study.

In addition to energies of nuclear states, we calculate a variety of other properties, such as one- and two-nucleon density and momentum distributions. An example is shown in Fig. 5 where the point proton and neutron densities of ${}^{4,6,8}\text{He}$ are shown. The α is extremely compact and has essentially identical proton and neutron densities. In the halo nuclei ${}^{6,8}\text{He}$ (so-called because of the weakly bound valence neutrons and consequently extended neutron distribution) the α core is only slightly distorted. However, the valence neutrons drag the center of mass of the α around and thus spread out the proton density. Recent neutral atom trapping experiments that measure the isotope shift of

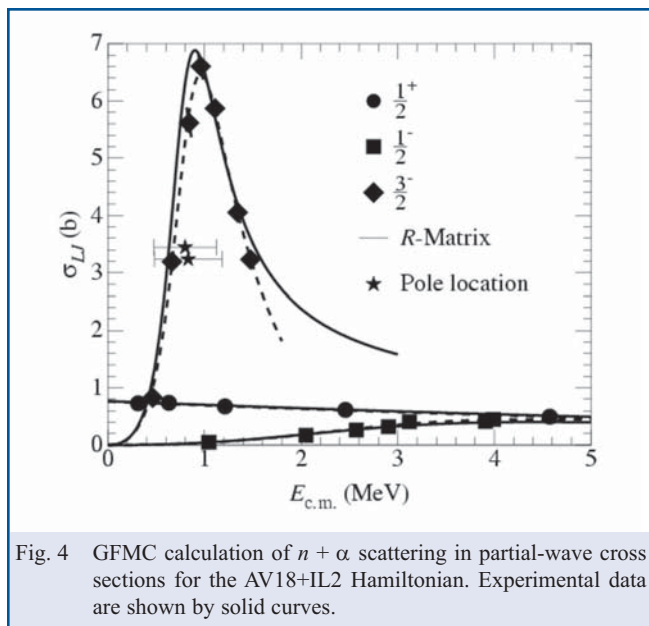


Fig. 4 GPMC calculation of $n + \alpha$ scattering in partial-wave cross sections for the AV18+IL2 Hamiltonian. Experimental data are shown by solid curves.

atomic transitions in these nuclei, combined with extremely accurate atomic theory, have determined the charge radius differences among the helium isotopes [25]. GPMC calculations of these charge radii are quite challenging because the neutron separation energies are only 1–2 MeV, so absolute energies of the ${}^4, {}^6, {}^8\text{He}$ nuclei must be calculated to much better than our standard 1–2% accuracy. By using variations of the AV18+IL2 Hamiltonian for the GPMC propagator, it is possible to map out the dependence of the charge radius on separation energy, and then read off a prediction from the experimental separation energy. The resulting radii agree with atom trap experiments at the 1-2% level [26].

CONCLUSIONS

The VMC and GPMC quantum Monte Carlo methods discussed here have established a new standard of comparison for the *ab initio* study of light nuclei using realistic interactions. There are many calculations of interest beyond those discussed here. These include the study of the small isovector and isotensor terms in the nuclear Hamiltonian, which contribute to the energy difference between “mirror” nuclei like ${}^3\text{H}$ – ${}^3\text{He}$ and ${}^7\text{Li}$ – ${}^7\text{Be}$. The microscopic origin of these forces is not fully understood, so the ability to test interaction models against experimental energies is an important tool.

Electromagnetic and weak transitions between different nuclear states and the response of nuclei to scattered electrons, neutrinos, and pions is also of considerable interest. The first GPMC calculations of magnetic dipole ($M1$), electric quadrupole ($E2$), and weak Fermi (F) and Gamov-Teller (GT) transitions in light nuclei are just becoming available [27]. VMC calculations have been made for the electromagnetic elastic and transition form factors in ${}^6\text{Li}$ [28] and for spectroscopic factors in the ${}^7\text{Li}(e, e'p)$ [29] reaction which are in good agreement with experiment. Calculations of spectroscopic amplitudes such as

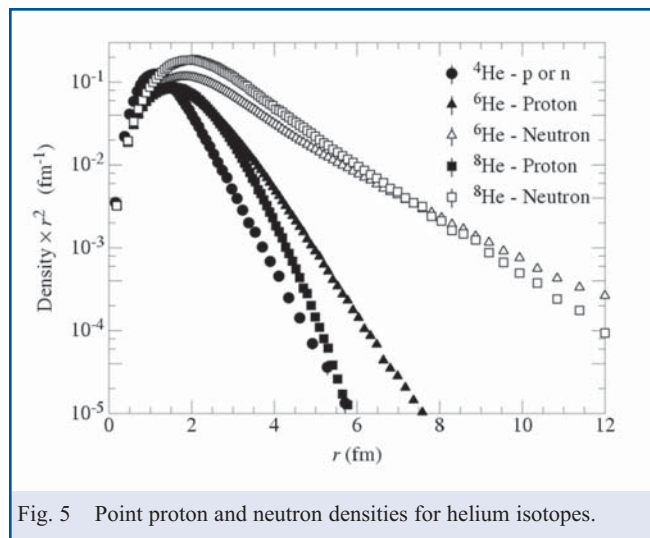


Fig. 5 Point proton and neutron densities for helium isotopes.

$\langle {}^8\text{Li}(J) + n(j) | {}^9\text{Li}(J') \rangle$, where the nuclei are in a number of different possible excited states, are being used as input to DWBA analyses of radioactive beam experiments, such as ${}^2\text{H}({}^8\text{Li}, p){}^9\text{Li}$ [30]. There have also been VMC studies of astrophysically interesting radiative capture reactions such as $d(\alpha, \gamma){}^6\text{Li}$, $t(\alpha, \gamma){}^7\text{Li}$, and ${}^3\text{He}(\alpha, \gamma){}^7\text{Be}$ [31]. GPMC calculations of such reactions should be feasible in the next few years.

The chief drawback of the present VMC and GPMC methods is the exponential growth in computational requirements with the number of nucleons. It will be some time before $A=11, 12$ calculations become routine. One of the challenges in moving to larger nuclei is the need to transition from parallel computers with hundreds of processors, to the next generation of massively parallel machines with tens of thousands of processors. With present machines tens of configurations reside on each processor, but in future one configuration might be spread over ten processors, which will require some major programming adjustments.

To reach larger nuclei, a new quantum Monte Carlo method, auxiliary field diffusion Monte Carlo (AFDMC), is under development and has already been used for larger nuclei like ${}^{16}\text{O}$ and ${}^{40}\text{Ca}$ using slightly simpler interactions [32]. The chief advantage of this method is that, by linearizing the problem with the introduction of auxiliary fields, spins and isospins can be effectively sampled, rather than completely summed over. The other *ab initio* nuclear many-body methods, NCSM and CCE, are also pushing on to larger nuclei, and we expect continued rapid progress in this field.

ACKNOWLEDGMENTS

The quantum Monte Carlo work described here has been done by many researchers including J. Carlson, K.M. Nollett, V.R. Pandharipande, M. Pervin, S.C. Pieper, B.S. Pudliner, R. Schiavilla, and K. Varga. This work is supported by the U.S. Department of Energy, Office of Nuclear Physics, under contract DE-AC02-06CH11357.

REFERENCES

1. J. Carlson and R. Schiavilla, *Rev. Mod. Phys.* **70**, 743-841 (1998), and references therein.
2. S.C. Pieper and R.B. Wiringa, *Annu. Rev. Nucl. Part. Sci.* **51**, 53-90 (2001), and references therein.
3. H. Kamada *et al.*, *Phys. Rev. C* **64**, 044001 (2001).
4. A. Kievsky *et al.*, *Phys. Rev. C* **58**, 3085 (1998).
5. A. Deltuva *et al.*, *Phys. Rev. C* **71**, 064003 (2005).
6. P. Navrátil, J.P. Vary and B.R. Barrett, *Phys. Rev. Lett.* **84**, 5728 (2000); P. Navrátil and W.E. Ormand, *Phys. Rev. Lett.* **88**, 152502 (2002), and references therein.
7. G. Hagen *et al.*, *Phys. Rev. C* **76**, 044305 (2007), and references therein.
8. V.G.J. Stoks *et al.*, *Phys. Rev. C* **49**, 2950 (1994).
9. R.B. Wiringa, V.G.J. Stoks, and R. Schiavilla, *Phys. Rev. C* **51**, 38 (1995).
10. R. Machleidt, F. Sammarruca, Y. Song, *Phys. Rev. C* **53**, R1483 (1996); R. Machleidt, *Phys. Rev. C* **63**, 024001 (2001).
11. J. Fujita and H. Miyazawa, *Prog. Theor. Phys.* **17**, 360 (1957); **17**, 366 (1957).
12. S.A. Coon, *et al.*, *Nucl. Phys.* **A317**, 242 (1979).
13. J. Carlson, V.R. Pandharipande, and R.B. Wiringa, *Nucl. Phys.* **A401**, 59 (1983).
14. S.C. Pieper, *et al.*, *Phys. Rev. C* **64**, 014001 (2001).
15. E. Epelbaum, *Prog. Part. Nucl. Phys.* **57**, 654 (2006), and references therein.
16. J. Lomnitz-Adler, V.R. Pandharipande, and R.A. Smith, *Nucl. Phys.* **A361**, 399 (1981).
17. J. Carlson, *Phys. Rev. C* **36**, 2026 (1987).
18. S.C. Pieper, K. Varga, and R.B. Wiringa, *Phys. Rev. C* **66**, 034611 (2002).
19. S.C. Pieper, *Nucl. Phys.* **A751**, 516c (2005).
20. R.B. Wiringa, *Phys. Rev. C* **43**, 1585 (1991).
21. N. Metropolis, *et al.*, *J. Chem. Phys.* **21**, 1087 (1953).
22. R.B. Wiringa, *et al.*, *Phys. Rev. C* **62**, 014001 (2000).
23. E. Caurier, *et al.*, *Phys. Rev. C* **66**, 024314 (2002).
24. K.M. Nollett, *et al.*, *Phys. Rev. Lett.* **99**, 022502 (2007).
25. L.-B. Wang, *et al.*, *Phys. Rev. Lett.* **93**, 142501 (2004); P. Mueller, *et al.*, *Phys. Rev. Lett.* **99**, 252501 (2007).
26. S.C. Pieper, *Proceedings of the "Enrico Fermi" Summer School Course CLXIX* (to be published); arXiv:0711.1500v1 [nucl-th].
27. M. Pervin, S.C. Pieper, and R.B. Wiringa, *Phys. Rev. C* **76**, 064319 (2007).
28. R.B. Wiringa and R. Schiavilla, *Phys. Rev. Lett.* **81**, 4317 (1998).
29. L. Lapidás, J. Wesseling, and R.B. Wiringa, *Phys. Rev. Lett.* **82**, 4404 (1999).
30. A.H. Wuosmaa, *et al.*, *Phys. Rev. Lett.* **94**, 082502 (2005).
31. K.M. Nollett, *Phys. Rev. C* **63**, 054002 (2001).
32. S. Fantoni, A. Sarsa, and K.E. Schmidt, *Phys. Rev. Lett.* **87**, 181101 (2001).